



Pectoral Muscle Segmentation in Tomosynthesis Images using Geometry Information and Grey Wolf Optimizer

Mohamed Abdel-Nasser^{1,2}^a, Francesc Porta Solsona¹ and Domenec Puig¹^b

¹Computer Engineering and Mathematics Department, University Rovira i Virgili, Tarragona, Spain

²Electrical Engineering Department, Aswan University, Aswan, Egypt

Keywords: Tomosynthesis, Breast Cancer, Pectoral Muscle, CAD Systems.

Abstract: Digital breast tomosynthesis (DBT) is quickly replacing full-field digital mammography because it allows a more efficient breast cancer diagnostic workflow and yields a more confident interpretation. The visual characteristics of the pectoral muscle on mediolateral oblique (MLO) views may increase the false positive rate in computer-aided diagnosis systems. Therefore, the pectoral muscle should be extracted from MLO images before further analysis. Notably, most pectoral muscle segmentation method has a fixed parameter setting that may yield good results with some images and fail with others due to the variations in breast density. In this paper, we propose a promising method to segment pectoral muscles from tomosynthesis images based on geometric information of the pectoral muscle and a meta-heuristic optimization algorithm. Concretely, our method involves four steps: 1) a preprocessing step, 2) obtaining of geometric information of pectoral muscle, 3) selection of pectoral muscle pixels, and 4) finding the optimal parameters using the grey wolf optimizer (GWO). The GWO optimizer gets different parameters for each input image as they depend on the visual characteristics of the images (i.e., breast density). With each input image, the GWO optimizer determines different values of the parameters because they rely on the visual characteristics of tomosynthesis images that are highly related to breast density. The proposed method is evaluated with a set of tomosynthesis images obtaining a Dice score of 0.823 and an IoU score of 0.726.


1 INTRODUCTION


Breast cancer is one of the common cancers occurring in women. Statistics reveal that the number of predicted deaths due to breast cancer in the European Union for the year 2019 is 92800 (Malvezzi et al., 2019). However, there is evidence that early diagnosis and treatment of breast cancer can significantly raise the probability of survival (Lee et al., 2010). Mammography (X-ray images of the breast) is, until now, the most useful tool for global population screening. However, the precise detection and diagnosis of a breast tumor completely based on mammography findings is hard and really depends on the expertise of the radiologist, which may yield a high number of false positives and extra screenings and examinations (Hubbard et al., 2011). Computer-aided detection and diagnosis (CAD) systems are already being adopted to help radiologists in the decision-making process (Abdel-Nasser et al., 2016a; Abdel-Nasser et al., 2016b). Such systems may highly de-

crease the amount of effort necessitated for the evaluation of a lesion in clinical practice while decreasing the number of false positives that may yield undesirable biopsies. Nowadays, digital breast tomosynthesis (DBT) is speedily succeeding in full-field digital mammography because it enables a more effective breast cancer diagnostic and produces a more trusting interpretation.

Breast masses are seen as white regions in mammograms. Hence CAD systems encounter difficulty when analyzing these images in the mediolateral oblique (MLO) view due to the appearance of the pectoral muscle, which has an appearance similar to the pixels of the breast region that increases the false positive rate in CAD systems. Therefore, the pectoral muscle should be removed from the breast region in MLO images before additional analysis. The higher number of images that need to be reviewed encounters a challenge for segmenting the pectoral muscle manually (a time-consuming task). One of the main steps of these CAD systems is the automated removal of pectoral muscle from mammograms and tomosynthesis images and leaving the breast region only.

It worth remarking that DBT images contain the

^a <https://orcid.org/0000-0002-1074-2441>

^b <https://orcid.org/0000-0002-0562-4205>

following kinds of pectoral muscles, namely, regular, convex, concave, and combinatorial. In the literature, numerous methods have been suggested to extract pectoral muscles. For example, in (Taghanaki et al., 2017a), geometric rules with a region growing algorithm are employed to segment pectoral muscles. Few publicly available mammographic image analysis tools, such as LIBRA (Keller et al., 2015) and OpenBreast (Pertuz et al., 2019), embrace the pectoral muscle segmentation step.

Most pectoral muscle segmentation method set a fixed parameter setting that may work with some images and fail with others due to the variations in the density of breasts. In this paper, we propose a promising method to automatically segment pectoral muscles from tomosynthesis images based on geometric information of the breast and a meta-heuristic optimization algorithm. Specifically, the proposed method comprises the following four steps: 1) a pre-processing step, 2) obtaining of geometric information of pectoral muscle, 3) selection of pectoral muscle pixels, and 4) finding the optimal parameters using the grey wolf optimizer (GWO). The GWO algorithm determines different parameters for each input image as they depend on the visual characteristics of the images (i.e., breast density). With each input image, the GWO optimizer determines different values of the parameters because they rely on the visual characteristics of tomosynthesis images that are highly related to breast density.

The remaining of this paper comprises the subsequent sections. Section 2 presents related work. Section 3 explains the proposed method. Section 4 presents the results. Section 5 summarizes the paper.

2 RELATED WORK

There are several pectoral muscle segmentation techniques, such as thresholding methods, active contours methods, K-means clustering methods, region growing methods, edge detection using Gabor filters methods, statistical region properties methods, and deep learning-based methods. Each of these methods has a different complexity that varies from highly sophisticated to low complex. Below, we present examples of these methods and explain how they address the problem of segmenting pectoral muscle.

In (Sreedevi and Sherly, 2015) and (Unni et al., 2018), a global threshold is used to estimate an initial pectoral muscle boundary, and a morphology-based boundary refinement algorithm is applied. The resulting pectoral muscle region is then segmented by a combination of global thresholding and connected

components methods. With a subset of 161 images from the mini-MIAS mammographic images dataset, (Sreedevi and Sherly, 2015) achieved an accuracy of 90.06% of based on visual observation of the correctness of segmented images. The use of intensity only for segmenting the pectoral muscle from the breast region cannot produce a precise segmentation in most cases. That happens because there is no significant variation in texture and intensity between the pectoral muscle tissue and the other tissues of the breast.

The authors of (Ergin et al., 2016) proposed a region growing algorithm, in which the positions of initial seeds for the pectoral muscle region are determined based on the intensity of the region. As the intensity cannot be effectively used for detecting complex textures such as muscles, (Taghanaki et al., 2017b) proposed to use a set of geometric rules and a region growing method to segment pectoral muscles. Using the MIAS and DDSM mammographic images datasets, they achieved segmentation accuracy of 95% and 94%, respectively. Based on the assumption that pectoral muscles are near the chest wall on the upper-right or the upper-left of mammographic images, the authors of (Selvathi and Poornila, 2018) used only a single seed for region growing algorithm. If the pectoral muscle is at right, they set the seed point into the last 5th column in the input images; otherwise, they set it set into (5th column of and 5th row). The pectoral muscle boundary is then refined using morphology operations.

Furthermore, line estimation methods are popular pectoral muscle segmentation approaches, in which a straight or a curve can represent the boundary of the pectoral muscle. Hough transform is one of the most popular line estimation method used for pectoral muscle segmentation. Based on the Canny edge detector, the authors of (Qayyum and Basit, 2016) proposed a method for removing the pectoral muscle region from mammograms. Firstly, a 3x3 median filter was used to reduce the noise in input images. Then, they segmented the initial pectoral muscle region by a combination of the Canny edge detector and the intensity of the region. The final pectoral muscle boundary was determined using a straight-line estimation method applied to the boundary. They achieved an accuracy of 93% accuracy with the mini-MIAS dataset. Besides, the authors of (Palkar and Agrawal, 2016) proposed a straight-line estimation method for removing the pectoral muscle from mammograms based on the fact that the pectoral muscle is at the upper-left region of the breast. In the case of the original images in which the chest wall is not on the left side of the image, they flipped them horizontally. Then, the position of the middle-top pixel of the image was

computed and connected to the lowest-left pixel of the rectangle approximating the pectoral muscle with the straight-line connecting these pixels taken as the pectoral muscle boundary. Finally, the pectoral muscle was segmented based on the approximated triangle of the pectoral muscle boundaries. With the MIAS dataset, they achieved an accuracy of 80%.

Shi et al. (Shi et al., 2018) used the four-class K-means clustering method to segment the pectoral muscles. First, they used a 5x5 median filter to reduce the noise in the images and normalized the image in order to enhance the contrast. Then, they clustered the pixels and assigned the potential pectoral muscle region candidate to the cluster with the highest intensity. Next, they employed a Hough transform method to extract the initial pectoral muscle boundary and refined the final boundary by a polynomial curve fitting method.

Pavan et al. (Pavan et al., 2019) used a Canny method for extracting the initial pectoral muscle region based on rules derived from the location of pectoral muscle in mammograms. To accurately segment the pectoral muscles, they used a contour growing technique with seeds defined based on the initial pectoral muscle boundary. With a private dataset (30 images), they achieved a mean Jaccard index of 0.92. Besides, Toz et al. (Toz and Erdogmus, 2018) used neighborhood relations and geometrical properties for locating the pectoral muscle region. As the pectoral muscle region often represented as a triangle with high but homogeneous intensity, an initial pectoral muscle region is determined using edge detection at angles of 30°–45°. The resulting pectoral muscle boundary was refined using a linear interpolation method to fill any missing boundaries. With a subset of 60 images from the INbreast dataset, they achieved a mean sensitivity of 95.6%, a false positive rate of 2.74%, and a false negative rate of 4.33%.

As shown above, almost all pectoral muscle segmentation method has a fixed parameter setting that may perform well with some images and fail with others due to the variations in the density of breasts. To address this point, in this paper, we propose the use of a GWO optimizer to determine the optimal parameters required for segmenting the pectoral muscle from the input image. Notably, GWO determines the different parameters for each input image as they depend on the visual characteristics of the images (i.e., breast density).

3 PROPOSED ALGORITHM

The proposed method comprises the following steps: 1) a preprocessing step, 2) obtaining of geometric information of pectoral muscle, 3) selection of pectoral muscle pixels and 4) finding the optimal parameters using the GWO optimizer.

3.1 Preprocessing of Tomosynthesis Images

The preprocessing stage of the proposed algorithm includes three main steps: removing the outliers, aligning the orientation of images, and determining the view of the images.

S1) Removing the Outliers: Figure 1 demonstrates that tomosynthesis images contain the breast region as well as outliers (small objects that exist in tomosynthesis images). To segment the breast region from other objects existing in images, we create a binary mask from the original image using a threshold of 100, select the most prominent object in it (which will presumably be the breast region), and suppress all other small objects. This produces a mask that will be smoothed and applied to the original image to obtain the breast region only. Note that this region will also contain the pectoral muscle that exists in MLO views only.

S2) Aligning the Orientation of Images: Tomosynthesis images could be left-oriented (the chest on the left side of the image) or right-oriented. Here we work with left-oriented images. As depicted in Figure 2, we create two 3x3 windows, one on the left side and one on the right side of the image. The one that has the greater mean of intensity values indicates the orientation of the image. If the image is right-oriented, the image and the mask of the breast area will be flipped. Note that in the case of right-oriented tomosynthesis images, the algorithm would not be able to determine correctly whether the view is craniocaudal (CC) or MLO, nor find the pectoral muscle if there is any.

S3) Determining the View of the Images: To check if the input image has CC or MLO view, we use prior information about the shape of the breast. In the case of CC views, the breast regions tend to have a semi-circular shape, while in the case of MLO views, the top part of the breast is almost has a vertical line shape. As shown in Figure 3, we set two points at the top part of the breast edge (p_1 and p_2), and then we find the slope of the line that connects p_1 with p_2 . If this slope is close to the vertical line slope, the view will be MLO. Differently, If this slope is close to the horizontal line slope, the view will be

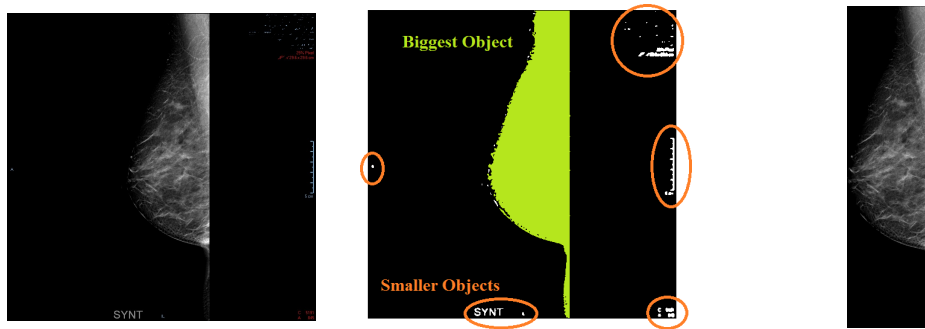


Figure 1: Preprocessing of tomosynthesis images. (a) original tomosynthesis image, (b) objects existing in the image, and (c) segmented breast region.

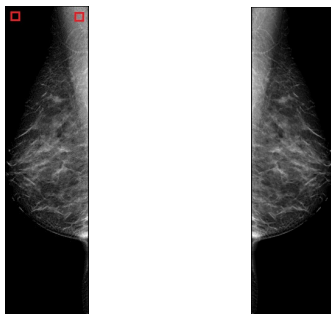


Figure 2: Aligning the orientation of images. (a) a 3x3 Windows, and (b) Flipped Image.

CC. Empirically, we set the slope limit to 45° . If the slope is higher than the limit, the view will be MLO; otherwise, CC. If the view is MLO, the next steps of the proposed method will be carried out; differently, and the algorithm will be terminated.

3.2 Obtaining of Geometric Rules

As shown in Figure 4, the edge of the pectoral muscle is located at the point A (the top of the image—first row of image). To find A , we compute the average of the intensities in the breast region for the first 30 rows of the image. Then, this average value is used as a threshold to create a binary image of the pixels with a higher intensity in the 10th-row region at the top of the image. As the images are prone to be affected by noise, we do not directly take the last white pixel on the first row in the mask, and we smooth the shape of this binary mask before locating where the edge is. To smooth the mask, we take the edge location of the first five rows and compute the mean of the column value of them, as it is still possible to find some essential variances in the mask even after the smoothing.

As depicted in Figure 5(a), we first determine the maximum inscribed circle (MIC) inside the breast region, by implementing the algorithm introduced in (Xia et al., 2007). The MIC algorithm applies a vec-

tor distance transformation to create a distance field, and an intensity value is set for each pixel of the image depending on the distance from that pixel to the edges of the breast. Then, it globally searches for the radius and center of the MIC. The center point O is determined by selecting the pixel with the highest intensity on the distance field, and the radius r is the distance from that pixel to the nearest edge point.

As shown in Figure 5(b), we determine the tangent line from A to MIC. We can express this process as follows:

- Calculate AO vector: $AO = (x_O - x_A, y_O - y_A)$
- Get middle point in AO : $C_2 = (\frac{AO_1}{2}, \frac{AO_2}{2})$

where C_2 is the center of a second circle with radius $\frac{AO}{2}$ that intersects with MIC in two points, and by solving the formulas of the two circles, we can get the intersections. It worth noting that the possible number of solutions (intersection points) of this problem are:

- Two intersection points (crossing circles).
- One intersection point (tangent circles).
- No intersection (separated circles).

As the line AO includes the radius of MIC, our case will always be the first case (two crossing circles with two intersection points). Therefore, we will choose the leftmost point (lower x value) and define it as point D . The line AD is extruded until it reaches the left edge of the image to find point B (see Figure 5(b)). This extrusion is made by calculating the straight line formula for AD $y = m * x + b$, where $m = \frac{\Delta y}{\Delta x} = \frac{y_A - y_D}{x_A - x_D}$ and $b = y_A - m * x_A$, and set $x_B = 1$ to find y_B using the same formula. Note that we need to find the point B to create the right-angled triangle. The point B is at the edge of the pectoral, in the first column. It is difficult to find B in the same way as A because, generally, the intensity of the pectoral pixels is more similar to the intensity of the breast ones due to the increasing density of the breast. Notably, a bit similar steps are employed in (Taghanaki, 2017).

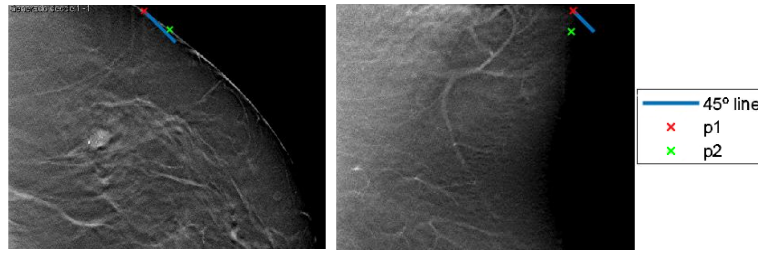


Figure 3: Determining the view of the images. (d) Binary mask over the breast and point A location.

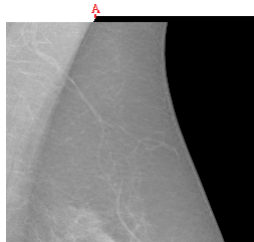


Figure 4: Obtaining of geometric rules.

3.3 Selection of Pectoral Muscle Pixels

We implement a region growing process inside the triangle previously defined by the geometrics of the breast. The starting seed point is placed near the center of this triangle to make sure that the seed is inside the pectoral region. The initial seed point is set to $(\frac{1}{4}A_x, \frac{1}{4}B_y)$. We formulate threshold of the selection as follows:

$$th = \bar{I}_{RG} - (dev) * \bar{I}_{RG} \quad (1)$$

where \bar{I}_{RG} is the average value of the intensities of the accepted pixels in the region growing process (only the seed at first iteration).

As noise may cause deviations in intensity values, and thus we do not calculate \bar{I}_{RG} from the intensities of pixels directly. Instead, we apply a mean filter by creating a 75×75 window around each pixel and compute the average of the intensities inside this window. Thus, \bar{I}_{RG} is defined as follows:

$$\bar{I}_{RG} = \sum_{i=1}^n \frac{\bar{p}x_i}{n} \quad (2)$$

here n is the number of pixels accepted in the region growing, and $\bar{p}x$ is the window average of a pixel.

$$\bar{p}x = \sum_{x,y=l1}^{x,y=l1} \frac{px(X+x, Y+y)}{75^2} \quad (3)$$

where $px(X, Y)$ is the intensity of the selected pixel, and x and y are the increments referring to the position inside the window, and we set $l1$ to 37.

In each iteration of the selection of pectoral muscle pixels, we perform the following:

- Select new pixel from the neighbour list (starts with seed).
- Recalculate \bar{I}_{RG} and th .
- Calculate the intensity $\bar{p}x$ of the selected pixel.
- Compare $\bar{p}x$ and th . If $\bar{p}x$ is higher, accept pixel and update n and the sum for \bar{I}_{RG} .
- Add neighbouring non-selected pixels to the neighbour list.

To add the neighboring pixels, we get the eight adjacent pixels around the selected pixel. In order to limit the method inside the geometry triangle and avoid adding the same pixel twice, we create a binary mask, as shown in Fig.6. We will mark neighboring pixels as zeros after adding them to the list, so if we mark a neighbor of the current iteration as zero, we will not include it again. The region growing process finishes when there are no more pixels in the neighbor list.

3.4 Determining the Optimal Parameters using the Grey Wolf Optimizer (GWO)

Note that AB is a straight-line approximation, but the edge of the pectoral muscle normally has a concave or convex shape. Concave pectorals will always inside the limit of the triangle, but for the convex ones, some pixels might be outside this limit. To avoid the under-segmentation of the pectoral muscle, we shift the line AB to the right by a factor δ from the top-left corner to B (see Figure 7). This is achieved by modifying the y-intercept term in the straight-line formula $b' = b + S$, where $S = \delta * B_y$, and recalculating the x' and y' of A' and B' , respectively.

Here, we use the GWO optimizer proposed in (Mirjalili et al., 2014) to find the optimal values of the shift δ of the line AB and the threshold parameter dev . The GWO optimizer simulates the social hierarchy of grey wolves, in order, alpha (α), beta (β), delta (Δ), and omega (ω) wolves. Alpha wolves are the leaders that manage and conduct the whole pack of wolves. They formulated the hunting mechanism

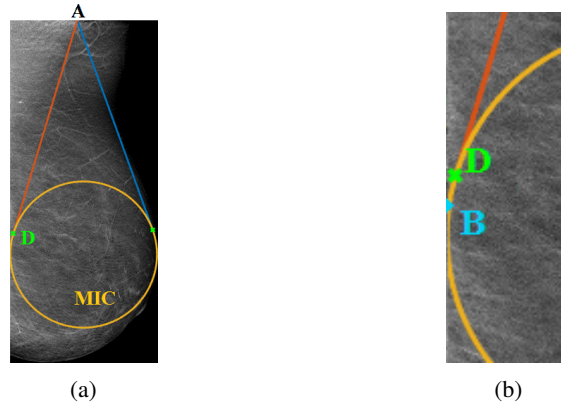


Figure 5: (a) A-MIC intersection points, (b) AD extrusion to point B.



Figure 6: Position of the seed over the binary mask.

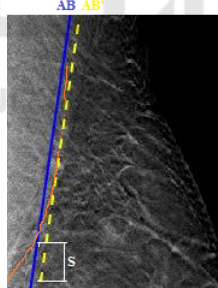


Figure 7: Original AB line and shifted AB' line (hand-drawn pectoral edge in orange).

of grey wolves using three steps: tracking and diminishing the prey, surrounding the prey until it stops, and hitting it. The prey encircling is expressed as follows:

$$\vec{D} = |\vec{C} \cdot \vec{X}_p(I) - \vec{X}| \quad (4)$$

$$\vec{X}(I+1) = \vec{X}_p(I) - \vec{A} \cdot \vec{D} \quad (5)$$

where I indicates the current iteration, \vec{A} and \vec{C} are coefficient vectors, $\vec{X}_p(I)$ is the position vector of the prey, \vec{X} refers to the position vector of a grey wolf, \vec{A} and \vec{C} can be calculated as $\vec{A} = 2\vec{a} \cdot \vec{r}_1 - \vec{a}$, $\vec{C} = 2\vec{r}_2$.

The wolf alpha guides the hunting process. Mirjalili et al. (Mirjalili et al., 2014) formulated this process as

$$D_\alpha = |C_1 \cdot X_\alpha - X| \quad (6)$$

$$D_\beta = |C_2 \cdot X_\beta - X| \quad (7)$$

$$D_\Delta = |C_3 \cdot X_\Delta - X| \quad (8)$$

where $\vec{X}_1 = \vec{X}_\alpha - \vec{A}_1 \cdot (\vec{D}_\alpha)$, $\vec{X}_2 = \vec{X}_\beta - \vec{A}_2 \cdot (\vec{D}_\beta)$, $\vec{X}_3 = \vec{X}_\Delta - \vec{A}_3 \cdot (\vec{D}_\Delta)$, and $\vec{X}(I+1) = (\vec{X}_1(I) + \vec{X}_2(I) + \vec{X}_3(I))/3$. Finally, they model the process of approaching and hunting the prey by decreasing the value of A randomly in the range $[-wd, wd]$, and reduce the value of wd from 2 to 0 over the iteration.

In our experiments, we set the search ranges of dev and δ , number of iteration, number of agents to $[0.3, 0.7]$, $[-1/4, 1/4]$, 10, and 5, respectively. We calculate the fitness of each search agent using the segmented pectoral regions. In this paper, we use entropy, which is a statistical measure of randomness. It can be used to characterize the texture of an image. Entropy is defined as follows:

$$E = -\sum(p_i \cdot \log_2(p_i)) \quad (9)$$

where p contains the normalized counts of the histogram of input image. The fitness function is expressed as follows:

$$fit = 1 - \frac{1}{entropy} \quad (10)$$

The Homogeneity measure the closeness of the distribution of the elements in the image. Homogeneity is defined as follows (Y. Li, H. Chen, Y. Yang, N. Yang, 2013):

$$H = \sum_{i=0}^{2^n} \sum_{j=0}^{2^n} \frac{1}{1 + (i-j)^2} \times p_t(i, j) \quad (11)$$

where $p_t(i, j)$ are the pixel intensities of the image, and the homogeneity fitness is expressed as follows:

$$fitH = 1 - homogeneity \quad (12)$$

In future studies, we will use an artificial neural network (Abdel-Nasser et al., 2018) instead of GWO to find the best parameters.

4 RESULT AND DISCUSSION

In our experiments, a total of 16 tomosynthesis images are employed to evaluate the performance of the proposed method. We gathered the images from a hospital in Spain (Hospital Universitario Puerta del Mar). This paper used manually segmented pectoral muscle regions as the ground-truth. Utilizing a computer graphic user interface (GUI) tool in MATLAB, we outlined pectoral muscle regions on tomosynthesis images in the dataset of this research.

In this study, we use two metrics for evaluating the efficacy of the proposed method: Dice and intersection-over-union (IoU). The Dice and IoU scores can be defined as follows:

$$\text{Dice} = \frac{2|Im_o \cap Im_s|}{|Im_o| + |Im_s|} \quad (13)$$

$$\text{Jaccard} = \frac{|Im_o \cap Im_s|}{|Im_o \cup Im_s|} \quad (14)$$

where R_o^i and R_s^i are the segmentation masks of the proposed method and the ground truth, respectively. The values of Jaccard and Dice metrics vary from 0 to 1. If any of the two metrics have a value of 0, it indicates that two masks have no common elements, while we obtain a value of 1 with Jaccard and Dice metrics if and only if the masks are identical. The larger the values of the Jaccard and Dice metrics, the more accurate the segmentation obtained by the proposed method.

In Table 1 we show the Dice of the IoU scores of the proposed method when using the Entropy and Homogeneity fitness function. As shown, the proposed method achieves the best results with the Homogeneity fitness function with Dice score of 0.823 and an IoU score of 0.726.

Table 1: Segmentation results of the proposed method.

| Fitness | Dice | IoU |
|---------------------|-------------------|-------------------|
| Entropy fitness | 0.816±0.11 | 0.702±0.15 |
| Homogeneity fitness | 0.823±0.09 | 0.726±0.13 |

Figure 8 shows an example of pectoral muscle segmentation in tomosynthesis images. Figure 8(a) shows the input tomosynthesis image, Figure 8(b) presents the binary mask generated by the proposed method. The binary mask is multiplied with the the input tomosynthesis image to suppress the pectoral muscle. As shown in Figure 8(c), the proposed method accurately segment the pectoral muscle from the breast area.

5 CONCLUSIONS

In this paper, we have presented a promising method for pectoral muscle segmentation from tomosynthesis images automatically. The proposed method includes four steps: 1) a preprocessing step, 2) obtaining of geometric information of pectoral muscle, 3) selection of pectoral muscle pixels, and 4) finding the optimal parameters using the grey wolf optimizer (GWO). The optimizer determines distinct parameters setting for each input image as they depend on its breast density. The proposed method is assessed with a set of tomosynthesis images and achieved a Dice score of 0.823 and an IoU score of 0.726. The future work will be focused on the use of various fitness function as well as evaluating the proposed with a larger dataset of tomosynthesis images.

ACKNOWLEDGEMENTS

This research was partly supported by the Spanish Government through project DPI2016-77415-R.

REFERENCES

- Abdel-Nasser, M., Mahmoud, K., and Kashef, H. (2018). A novel smart grid state estimation method based on neural networks. *IJIMAI*, 5(1):92–100.
- Abdel-Nasser, M., Moreno, A., and Puig, D. (2016a). Temporal mammogram image registration using optimized curvilinear coordinates. *Computer methods and programs in biomedicine*, 127:1–14.
- Abdel-Nasser, M., Saleh, A., Moreno, A., and Puig, D. (2016b). Automatic nipple detection in breast thermograms. *Expert Systems with Applications*, 64:365–374.
- Ergin, S., Esener, İ. I., and Yüksel, T. ((2016)). A genuine glcm-based feature extraction for breast tissue classification on mammograms. *International Journal of Intelligent Systems and Applications in Engineering*, pages 124–129.
- Hubbard, R. A., Kerlikowske, K., Flowers, C. I., Yankaskas, B. C., Zhu, W., and Miglioretti, D. L. (2011). Cumulative probability of false-positive recall or biopsy recommendation after 10 years of screening mammography: a cohort study. *Annals of internal medicine*, 155(8):481–492.
- Keller, B. M., Chen, J., Daye, D., Conant, E. F., and Kontos, D. (2015). Preliminary evaluation of the publicly available laboratory for breast radiodensity assessment (libra) software tool: comparison of fully automated area and volumetric density measures in a case-control study with digital mammography. *Breast Cancer Research*, 17(1):117.

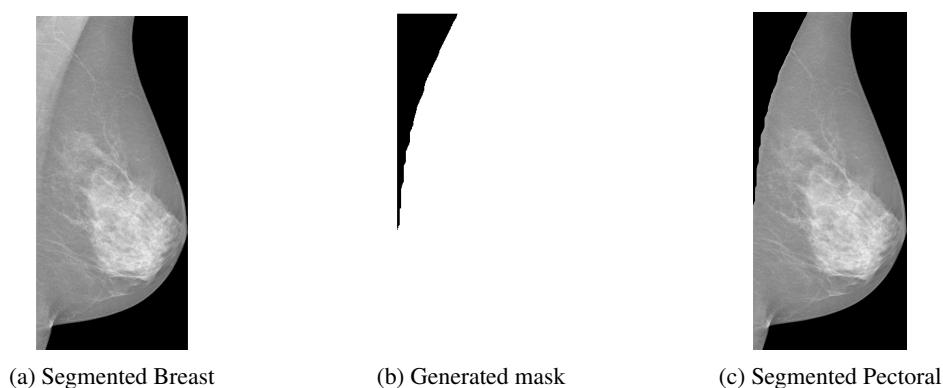


Figure 8: Example of pectoral muscle segmentation result.

- Lee, C. H., Dershaw, D. D., Kopans, D., Evans, P., Monsees, B., Monticciolo, D., Brenner, R. J., Bassett, L., Berg, W., Feig, S., et al. (2010). Breast cancer screening with imaging: recommendations from the society of breast imaging and the acr on the use of mammography, breast mri, breast ultrasound, and other technologies for the detection of clinically occult breast cancer. *Journal of the American college of radiology*, 7(1):18–27.
- Malvezzi, M., Carioli, G., Bertuccio, P., Boffetta, P., Levi, F., La Vecchia, C., and Negri, E. (2019). European cancer mortality predictions for the year 2019 with focus on breast cancer. *Annals of Oncology*, 30(5):781–787.
- Mirjalili, S., Mirjalili, S. M., and Lewis, A. (2014). Grey wolf optimizer. *Advances in engineering software*, 69:46–61.
- Palkar, P. and Agrawal, P. (2016). A technique to extract statistical parameters of digital mammogram to detect breast cancer. *Int. J. Adv. Res. Sci. Eng. Technol.*, 3(12):3033–3038.
- Pavan, A. L., Vacavant, A., Alves, A. F., Trindade, A. P., and de Pina, D. R. ((2019)). Automatic identification and extraction of pectoral muscle in digital mammography. In *World Congress on Medical Physics and Biomedical Engineering 2018*, pages 151–154. Springer.
- Pertuz, S., Torres, G. F., R., T., and Kamarainen, J. (2019). Open framework for mammography-based breast cancer risk assessment. In *IEEE-EMBS International Conference on Biomedical and Health Informatics*.
- Qayyum, A. and Basit, A. ((2016)). Automatic breast segmentation and cancer detection via svm in mammograms. In *2016 International conference on emerging technologies (ICET)*, pages 1–6. IEEE.
- Selvathi, D. and Poornila, A. A. ((2018)). Deep learning techniques for breast cancer detection using medical image analysis. In *Biologically Rationalized Computing Techniques For Image Processing Applications*, pages 159–186. Springer.
- Shi, P., Zhong, J., Rampun, A., and Wang, H. ((2018)). A hierarchical pipeline for breast boundary segmentation and calcification detection in mammograms. *Computers in biology and medicine*, 96:178–188.
- Sreedevi, S. and Sherly, E. ((2015)). A novel approach for removal of pectoral muscles in digital mammogram. *Procedia Computer Science*, 46:1724–1731.
- Taghanaki, S. A., L. Y. M. B. H. (2017). Geometry-based pectoral muscle segmentation from mlo mammogram views. *IEEE Transactions on Biomedical Engineering*, 64(11):2662–2671.
- Taghanaki, S. A., Liu, Y., Miles, B., and Hamarneh, G. (2017a). Geometry-based pectoral muscle segmentation from mlo mammogram views. *IEEE Transactions on Biomedical Engineering*, 64(11):2662–2671.
- Taghanaki, S. A., Liu, Y., Miles, B., and Hamarneh, G. ((2017)b). Geometry-based pectoral muscle segmentation from mlo mammogram views. *IEEE Transactions on Biomedical Engineering*, 64(11):2662–2671.
- Toz, G. and Erdogmus, P. ((2018)). A single sided edge marking method for detecting pectoral muscle in digital mammograms. *Eng Technol Appl Sci Res*, 8:2367–2373.
- Unni, A., Eg, N., Vinod, S., and Nair, L. S. ((2018)). Tumour detection in double threshold segmented mammograms using optimized glcm features fed svm. In *2018 International Conference on Advances in Computing, Communications and Informatics (ICACCI)*, pages 554–559.
- Xia, R., Liu, W., Zhao, J., Bian, H., and Xing, F. (2007). Robust algorithm for detecting the maximum inscribed circle. In *2007 10th IEEE International Conference on Computer-Aided Design and Computer Graphics*, pages 230–233. IEEE.
- Y. Li, H. Chen, Y. Yang, N. Yang (2013). Pectoral muscle segmentation in mammograms based on homogenous texture and intensity deviation. *ELSEVIER*, 46(Issue 3):681–691.